

## IR-REMPI of vanadium-carbide nanocrystals: Ideal versus truncated lattices

Gert von Helden <sup>a,\*</sup>, Deniz van Heijnsbergen <sup>a</sup>, Michael A. Duncan <sup>c</sup>,  
Gerard Meijer <sup>a,b</sup>

<sup>a</sup> FOM-Institute for Plasmaphysics Rijnhuizen, Edisonbaan 14, NL-3439 MN Nieuwegein, The Netherlands

<sup>b</sup> Department of Molecular and Laser Physics, University of Nijmegen, Toernooiveld 1, NL-6525 ED Nijmegen, The Netherlands

<sup>c</sup> Department of Chemistry, University of Georgia, Athens, GA 30602, USA

Received 21 August 2000; in final form 30 October 2000

### Abstract

Neutral vanadium-carbide clusters are produced in the gas phase with laser vaporization in a pulsed nozzle source and excited with a free electron laser in the 400–1000 cm<sup>-1</sup> region. Resonant multiphoton excitation induces thermionic electron emission in the isolated metal carbide nanocrystals. This process only occurs for stable neutral clusters which resist multiphoton dissociation. The species observed are cubic nanocrystals and truncated nanocrystals with carbon vacancies at their corners. Their wavelength spectra exhibit resonances associated with surface phonons. The resonance shows only a weak size dependence, shifting from 530 to 490 cm<sup>-1</sup> in going from V<sub>14</sub>C<sub>12</sub> to V<sub>32</sub>C<sub>32</sub>. © 2001 Elsevier Science B.V. All rights reserved.

### 1. Introduction

Atomic clusters composed of metals, semiconductors and carbon exhibit remarkable chemical and physical properties. New techniques have made it possible to prepare metal [1,2] or semiconductor clusters [3–5] in macroscopic amounts in solution or deposited on surfaces. Quantum confinement and interfacial effects produce novel properties suggesting many new applications. Some clusters also occur naturally, for example titanium-carbide clusters have recently been identified in the surroundings of dying stars [6]. The structures of condensed or supported clusters of-

ten adopt ‘nanocrystal’ structures with ordered lattices. In some systems, the finite lattices in nanocrystals have the same symmetry as the corresponding bulk material, while in others the nucleation dynamics produce metastable configurations. However, many interesting clusters can only be produced in the low density gas phase, and the measurement of their properties is more problematic. Unlike condensed or supported clusters, the structures of gas phase clusters are the subject of much speculation. One exception to this occurs for the metal compound clusters, where ‘magic numbers’ at certain cluster sizes and stoichiometries provide strong evidence for nanocrystal structures [7–10]. In this report, we investigate thermionic electron emission for gas phase vanadium-carbide nanocrystals using resonance-enhanced absorption of multiple infrared

\* Corresponding author. Fax: +31-30-6031204.

E-mail address: gertvh@rijnh.nl (G. von Helden).

photons, a technique we denote as IR-REMPI. IR-REMPI is confirmed as a selective method to identify stable neutral clusters, and fascinating insights into the structures of vanadium-carbide nanocrystals are obtained.

Magic numbers in cluster size and composition may result from the thermodynamics and kinetics of cluster growth, where multiple addition, rearrangement and fragmentation events lead to the predominant survival of stable species. For charged clusters, the species produced may be measured directly in mass spectrometers. However, measurements on neutral clusters require their ionization for detection. This is usually accomplished with photoionization, in which ionization potentials, cross-sections and/or fragmentation processes provide unwanted complexity in mass spectra. Consequently, there is often confusion about magic numbers in mass spectra and the roles of neutral versus cation stability and it is generally not possible to determine the stability of neutrals present in a cluster distribution. A general technique to identify stable neutral clusters is thus clearly needed.

Our initial results on several cluster systems suggest that thermionic emission via IR-REMPI may be a convenient technique to detect stable neutrals. In most ionization schemes, *electronic* excitations access the ionization continuum. In thermionic emission, however, ionization occurs by coupling highly excited *vibrational* levels in the ground electronic state to the ionization continuum. In many molecules, the excitation exceeds the ground state dissociation limit before ionization can occur, and photodissociation is efficient. However, in strongly bound molecules such as atomic clusters, the ionization potential may be low and the dissociation energy high. Electron emission may therefore be competitive with dissociation in such systems. Thermionic emission induced by multiphoton absorption of ultraviolet or visible radiation has been observed previously for metal clusters [11,12], fullerenes [13,14] and small metal carbides [11,15,16]. In a recent work, we have shown that thermionic emission may also be induced by infrared radiation, and that in the case of  $C_{60}$ , this process only occurs on resonances in the known IR-absorption spectrum

[17,18]. This method was then applied to titanium-carbide clusters, whose IR spectra were previously unknown [6,19]. Different spectra were obtained for clusters believed to have different structures, and the resonances matched the theoretical predictions for vibrational spectra. These measurements suggest that IR-REMPI may become a general tool for the detection of stable neutral clusters and the measurement of their vibrational spectra. However, additional measurements are needed to confirm the generality and reliability of the method.

Here we extend these IR-REMPI studies to vanadium-carbide clusters. Early mass spectroscopy studies [20–22] on Ti, V and other transition metal carbide clusters showed that the mass  $M_8C_{12}^+$  is produced with extremely high abundance. Castleman proposed a cage structure with alternating metal atoms and  $C_2$  groups and coined the term ‘met-cars’ to indicate these clusters. Later, Duncan and co-workers showed that larger M/C ions have similar high abundance [8,9]. In particular, clusters with the 14/13 stoichiometry (i.e.,  $M_{14}C_{13}$ ) were proposed to be fragments of a face-centered-cubic (fcc) lattice [8,9] and termed nanocrystals. The initial structural assignment was supported by theory [23–25]. Recently, we observed the thermionic emission for titanium-carbide met-car clusters [19] and nanocrystals [6]. In these clusters, magic numbers were observed for the 8/12, 14/13, and larger nanocrystal stoichiometries, confirming that these species are stable neutral clusters. Nanocrystals were recognized by their (near) 1:1 stoichiometry and their correspondence to symmetric  $3 \times 3 \times 3$ ,  $3 \times 3 \times 4$ ,  $4 \times 4 \times 4$ , etc., fcc structures. IR-REMPI spectra were very different for the  $Ti_8C_{12}$  and the nanocrystal clusters, providing the first insight into their structures. However, the exact masses for larger nanocrystal masses for  $Ti_xC_y$  clusters were obscured because of the titanium isotopic distribution and the coincidence of  $^{48}Ti$  with four carbon atoms. Vanadium exhibits the same carbide cluster mass distribution as titanium in the previous work, but it is a single-isotope metal and precise stoichiometry measurements should be possible for larger clusters. These studies make it possible to investigate the generality of the IR-REMPI method, to compare

clusters of different metals and to measure the vibrational spectra as a function of cluster size.

## 2. Experimental

A schematic of the experiment is shown in Fig. 1. The clusters are generated by pulsed laser vaporization of a rotating and translating vanadium rod at 532 nm. A mixture of 5% CH<sub>4</sub> in argon from a pulsed valve entrains the plasma, clustering occurs, and the gas is expanded in vacuum. The molecular beam is skimmed, and any ions from the source are blocked using deflection plates located upstream from the mass spectrometer. The neutral beam then enters the interaction region with the IR laser, which is situated between the extraction plates of a reflectron time-of-flight (TOF) mass-spectrometer. The output of the free-electron laser FELIX [26] comes in macropulses of 5  $\mu$ s width at a repetition rate of 10 Hz. Each macropulse contains a series of 0.5–5 ps micro-pulses at a repetition rate of 1 GHz. A macropulse contains up to 100 mJ of energy and the bandwidth is transform limited. The tuning range is 40–2000 cm<sup>-1</sup>, although only the region from 400 to 1000 cm<sup>-1</sup> is used in the present experiments. The IR beam is focused on the molecular beam and fires at a time to intersect the molecular beam in the TOF source. Typically 5  $\mu$ s after the IR laser pulse, the TOF acceleration plates are pulsed to

high voltage and a TOF mass spectrum is recorded. Ionization can also be accomplished with the 248 nm light of a KrF excimer laser. In this case, the unfocused (several mJ) light is overlapped with the cluster beam.

## 3. Results and discussion

Fig. 2 shows the vanadium-carbide cluster mass spectrum obtained with ultraviolet light compared to that measured with infrared light. In Fig. 2A, the mass spectrum measured with a KrF excimer laser (248 nm) is shown. The largest peak corresponds to the V<sub>14</sub>C<sub>13</sub> cluster, and there are other abundant peaks at larger nanocrystal masses. This spectrum is consistent with that seen previously by photoionization and it is similar to the spectrum reported for ions sampled directly from the cluster source [8]. In Fig. 2B, a mass spectrum is shown that is obtained when using IR ionization and summing mass spectra while FELIX is scanned over the 400–1000 cm<sup>-1</sup> region. These spectra have several peaks in common, with the most prominent masses corresponding to the previously noted nanocrystals. However, while the UV spectrum has many additional peaks at intermediate masses, the IR spectrum is much cleaner. It has prominent peaks only at masses corresponding exactly to nanocrystals (e.g., 14/13) or to those in the immediate vicinity of nanocrystal stoichiometries. In

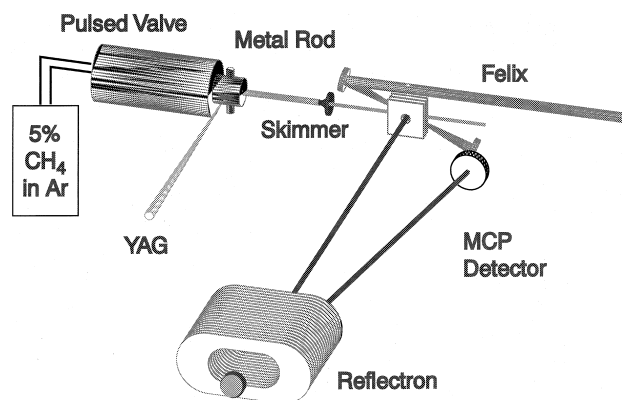


Fig. 1. Scheme of the experimental setup. Clusters are generated in a laser vaporization source. IR excitation occurs in a differentially pumped chamber. Ions produced are then mass analyzed in a reflectron time-of-flight mass spectrometer.

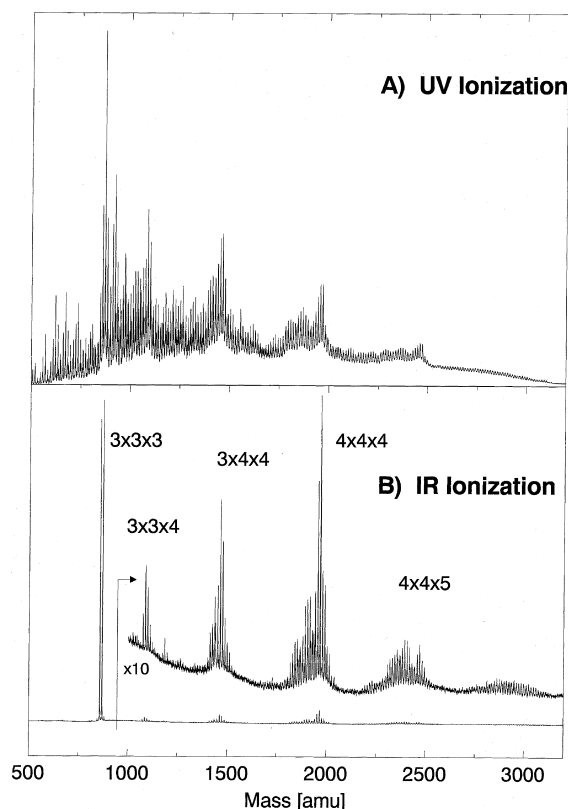


Fig. 2. Mass spectrum obtained when ionizing vanadium-carbide clusters with UV (KrF, 248 nm) radiation (A) and IR radiation (B). The IR ionization spectrum shown is the result from adding up spectra while tuning the IR laser from 400 to 1000  $\text{cm}^{-1}$ .

the IR spectrum, all mass peaks result from the multiple absorption of photons, followed by the thermionic emission of an electron. Spectra are taken at reduced IR fluences, and no change in the relative intensities in the spectrum is observed. The different peaks observed are therefore not caused by fragmentation during/after IR excitation. Thus, all masses observed must result from neutral species that evaporate an electron rather than a neutral fragment, i.e., species that are stable and resilient towards dissociation. Using UV ionization, many more mass peaks are observed, and there is a complex variation in relative intensities with laser power. This is probably caused by the reduced selectivity of UV ionization. Using UV ionization, all clusters with an ionization potential

below 5.0 eV can be ionized, and multiphoton absorption and fragmentation may also occur. In the case of IR ionization, the ionization efficiency will also depend on the ionization potential – with lower IP clusters ionizing more readily – but in addition also on cluster stability. In less stable clusters, fragmentation occurs before ionization, and smaller neutrals are produced which are not detected. Thus, only the most stable neutral species which survive the multiphoton absorption are ionized. Unlike UV ionization, then, IR-REMPI is intrinsically biased to detect the most stable neutral clusters.

The largest peak in Fig. 2B is found at a mass of 869.3 amu with an almost equally intense peak 12 amu lower. The cluster stoichiometries giving rise to these ion peaks are  $\text{V}_{14}\text{C}_{13}$  and  $\text{V}_{14}\text{C}_{12}$ , respectively. As described previously [8,9], a cube consisting of  $3 \times 3 \times 3$  atoms gives rise to the 14/13 composition. The peak 12 amu below may result from a  $3 \times 3 \times 3$  nanocrystal with the central carbon atom missing. Only these two peaks are seen at the  $3 \times 3 \times 3$  nanocrystal size, and these are by far the most abundant species detected. However, weaker peaks are found at larger nanocrystal sizes, and these peaks appear in groups. The largest peak in each group always occurs close to the stoichiometry expected for crystallites with  $3 \times 3 \times 4$ ,  $3 \times 4 \times 4$ ,  $4 \times 4 \times 4$ ,  $4 \times 4 \times 5$ , etc., atoms. The exact stoichiometries are verified using  $^{13}\text{CH}_4$  as the source of carbon.  $\text{V}_8\text{C}_{12}$  clusters are not observed here because the cluster source is optimized to produce nanocrystals and the IR laser is not scanned over the wavelength range where  $\text{M}_8\text{C}_{12}$  clusters have resonances [19]. Under other conditions,  $\text{V}_8\text{C}_{12}$  is detected, as expected. However, no evidence is found under any conditions for the presence of multi-cage structures which have been proposed previously [27].

Essentially every peak in the IR-REMPI mass spectrum can be assigned to nanocrystal stoichiometries or to formulas just below an exact nanocrystal. In Fig. 3, an expanded view of the four nanocrystal mass regions from Fig. 2B is given. In Fig. 3A, the region from 835 to 1235 amu is shown, with the peaks of  $\text{V}_{14}\text{C}_{13}$  and  $\text{V}_{14}\text{C}_{12}$  off-scale. Near 1100 amu, a second progression of

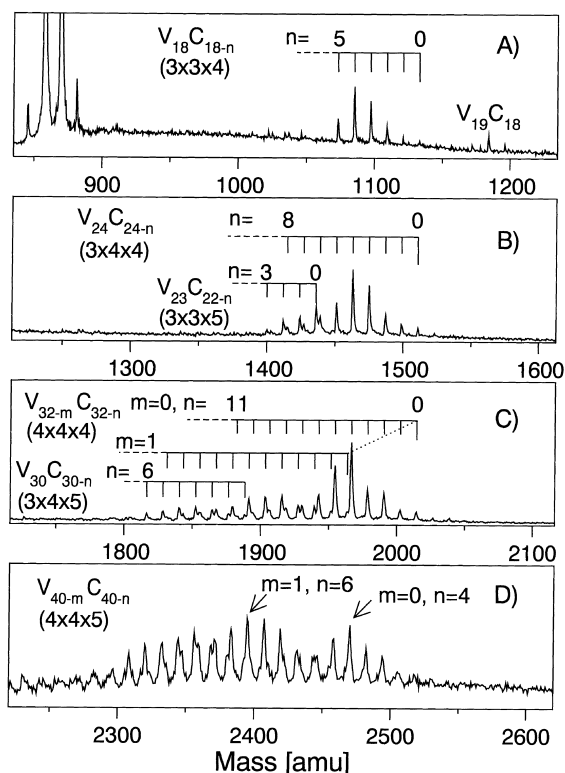


Fig. 3. Expanded views of the mass spectrum shown in Fig. 2B).

peaks is observed spaced by 12 amu, starting on the high mass side with the very weak mass peak of  $V_{18}C_{18}$ . The most intense peak corresponds to a structure having four carbon atoms less than 18/18, and no peaks belonging to this progression are observed below  $V_{18}C_{13}$ .  $V_{18}C_{18}$  is exactly the composition of a crystallite of  $3 \times 3 \times 4$  atoms and the peaks at the lower mass can reasonably be assumed to belong to the same structural family. At a 50.9 amu higher mass, a  $V_{19}C_{18}$  peak is observed which will be discussed later. In Fig. 3B, the region around mass 1500 is shown, where two progressions of peaks are assigned. The most intense series results from clusters with a composition  $V_{24}C_{24-n}$ , which begins at  $n=0$ , reaches its maximum at  $n=4$ , and goes out to about  $n=8$ . The other series stems from  $V_{23}C_{22-n}$  clusters. Here, the maximum intensity is found at  $n=0$  while the cluster intensity drops towards lower masses.  $V_{24}C_{24}$  corresponds to nanocrystal clusters

with  $3 \times 4 \times 4$  atoms, while  $V_{23}C_{22}$  corresponds to the  $3 \times 3 \times 5$  atom cluster. In Fig. 3C, three series of peaks are assigned. The two series at higher masses correspond to clusters of the composition  $V_{32-m}C_{32-n}$  with  $m=0$  and 1, while the lower mass distribution results from the  $V_{30}C_{30-n}$  clusters. All distributions start at  $n=0$  and their maxima occur at  $n=4$  for the first two and at  $n=3$  for the third, with  $n=4$  almost equal in intensity. The two distributions starting at higher masses result from  $4 \times 4 \times 4$  atom crystallites, while the lower mass distribution corresponds to the  $3 \times 4 \times 5$  crystallite. Near 2400 amu, shown in Fig. 3D, the cluster distribution becomes more complicated. However, all peaks observed can be assigned to clusters with a stoichiometry  $V_{40-m}C_{40-n}$ . The highest mass with  $m=0$  and  $n=0$  is exactly the composition expected for a  $4 \times 4 \times 5$  atom crystallite. Again, a local maximum is observed at  $m=0, n=4$ . The overall maximum in this distribution occurs for  $m=1, n=6$  with another maximum occurring at  $m=2, n=5$ .

It is evident from Fig. 3 that all mass peaks appear in progressions, indicating that the corresponding clusters do indeed belong to the same structural families. For most nanocrystals the ideal stoichiometry is observed, but carbon deficient clusters are often more abundant. Only two progressions, the one from the  $3 \times 3 \times 3$  atom and from the  $3 \times 3 \times 5$  atom cluster, show a maximum at the ideal stoichiometry expected for these nanocrystals. The other progressions from the  $3 \times 3 \times 4$ ,  $3 \times 4 \times 4$ ,  $3 \times 4 \times 5$ ,  $4 \times 4 \times 4$  and the  $4 \times 4 \times 5$  atom clusters show maxima at compositions with four (three for the  $3 \times 4 \times 5$  atom cluster) carbon atoms less than the ideal structure. This observation is the consequence of the possible atomic arrangements in such crystallite clusters, and serves as further evidence for their structure. In the  $3 \times 3 \times 3$  clusters, two arrangements of atoms are possible. One structure contains 14 metal and 13 carbon atoms, and the other 13 metal and 14 carbon atoms. Metal atoms occupy the corners of the 14/13 cube, whereas carbon atoms do so in the 13/14 structure. In the experiment, the 14/13 cluster is exclusively observed. The same holds for the  $3 \times 3 \times 5$  cluster, where also only the 23/22 species, which has metal atoms at the corners, is

observed. In contrast to these nanocrystals which have the most intense peak at the ideal stoichiometry, the ones which show the most intensity for lower masses are those which cannot have metal at all corners. When a crystallite contains one or more edges with an even number of atoms, the alternation of atoms requires that all corners cannot be occupied by the same type of atom. Instead, for the species under consideration here, four corners must be occupied by metal and the four remaining ones by carbon. Strikingly, all nanocrystals that have one or more edges with an even number of atoms show the most intense ion peak at a mass that corresponds to four carbon atoms less than the ideal structure. It thus seems very likely that these are the four carbon atoms that normally would occupy the corners of the crystallite. This suggests that it is intrinsically unfavorable to have carbon atoms at the corner sites of these nanocrystals. *Truncated* nanocrystals without these carbon atoms are apparently produced. While metal isotope distributions precluded a clear picture of this for titanium-carbide clusters, those masses which could be measured were consistent with a similar formation of carbon-deficient nanocrystals for even-dimension species [6,8,19].

The instability for carbon at corner sites is understandable. Because these sites allow only partial binding and strain occurs in the bonds, the bonding for either vanadium or carbon atoms will be less favorable here than it is for edges, faces or the interior. A difference between carbon and vanadium is, however, that vanadium uses *d*-electrons in its binding. This makes it more flexible, and vanadium is therefore expected to tolerate the strain at the corners better than carbon. Related to this, nanocrystal structures for titanium-carbide cluster *anions* have been proposed in which carbon atoms at the corners are replaced by  $C_2$  units [28]. Some clusters here also are missing one vanadium atom. Most likely, the vanadium vacancy is then at one of the corners of the crystallite. There appears to be a tendency for additional carbon vacancies when there is such a vanadium vacancy.

An interesting case is the  $V_{18}C_{18}$   $3 \times 3 \times 4$  atom nanocrystal. Here all four carbon corner atoms are located on the same  $3 \times 3$  atom face of the crystal. The maximum ion intensity results from the cluster

that has four carbon atoms less than the ideal structure. If our structural hypothesis is correct, then this cluster has only one carbon atom on this face. Interestingly, at the mass corresponding to that of the cluster lacking five carbon atoms, a discontinuity is observed in the mass spectrum – no mass peaks belonging to this series are observed to lower masses. It thus seems reasonable that those five carbon atoms are all missing from this one face. The peak that corresponds to the perfect  $3 \times 3 \times 4$  atom nanocrystal is rather weak. However, a more intense peak is observed exactly one vanadium mass higher. One can speculate that this  $V_{19}C_{18}$  peak results from a  $3 \times 3 \times 4$  atom where the face with the four carbon atoms at the corners is capped by a vanadium atom, which apparently stabilizes the otherwise loosely bound carbon atoms on this face.

While these mass spectra provide circumstantial evidence about cluster structures, additional information can be found in the wavelength dependence of the IR-REMPI signal. For titanium-carbide clusters, it was shown that  $Ti_{14}C_{13}$  has its main resonance near  $500\text{ cm}^{-1}$  [19], and that its peak positions agree very well with the IR active surface phonon modes of bulk TiC [29]. If these clusters are indeed ideal or truncated nanocrystals, they should have similar resonances. However,  $Ti_8C_{12}$  and  $Ti_8C_{11}$  clusters, which were calculated to have caged structures with surface  $C_2$  groups, have resonances near  $1400\text{ cm}^{-1}$  [19]. To investigate these structural possibilities further, we recorded the wavelength spectra for each peak in the mass spectrum. Fig. 4 shows these spectra for selected clusters. In Fig. 4A, the spectra of the  $V_{14}C_{13}$  ( $3 \times 3 \times 3$ ) and  $V_{14}C_{12}$  ( $3 \times 3 \times 3 - C$ ) clusters are shown. Both have strong resonances near  $500\text{ cm}^{-1}$ , but no resonance near  $1400\text{ cm}^{-1}$ . The two peaks clearly occur at different positions, with the peak of  $V_{14}C_{12}$  being shifted about  $20\text{ cm}^{-1}$  to the blue, compared to  $V_{14}C_{13}$ . Similar spectra are obtained for all the larger clusters. In Fig. 4B, the wavelength spectrum of the  $3 \times 3 \times 4$  clusters is shown. Analyzing the spectra of the three strongest mass peaks in this series showed that these spectra are indistinguishable and the sum of these three spectra is therefore shown. The peak is shifted several  $\text{cm}^{-1}$  to the red compared to

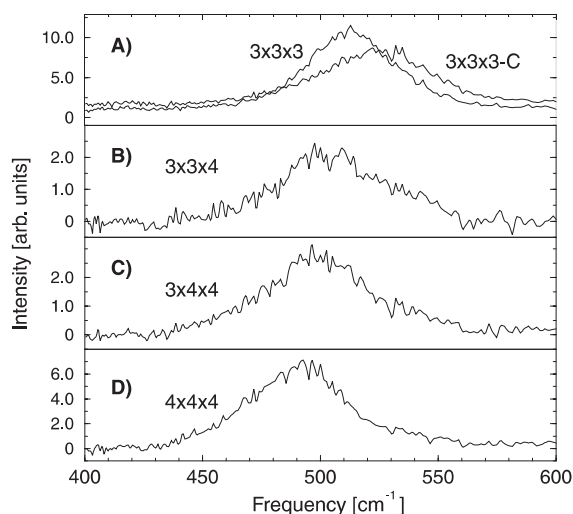


Fig. 4. Ion yield on specific vanadium-carbide clusters as a function of IR laser frequency. Shown in (A) is the spectrum of  $3 \times 3 \times 3$  and the  $3 \times 3 \times 3 - 12$  amu cluster. In (B)–(D) the spectra of the  $3 \times 3 \times 4$ ,  $3 \times 4 \times 4$  and  $4 \times 4 \times 4$  atom clusters are shown.

the  $3 \times 3 \times 3$  peak. In Figs. 4C and D, the wavelength spectra of the  $3 \times 4 \times 4$  and  $4 \times 4 \times 4$  series are shown. Again, the spectra from individual masses are found to be indistinguishable and are added up. A gradual shift of the peak positions to the red is again observed going from the small clusters to these larger ones. However, the most telling information about these spectra is their similarity. All clusters have resonances near  $500 \text{ cm}^{-1}$ , just as we found for the titanium-carbide nanocrystals. Surface phonon spectra for VC are not available for comparison, but the similarity to the TiC surface phonons is probably not a coincidence. Furthermore, these clusters have no resonances at higher frequencies characteristic of surface  $\text{C}_2$  groups. It thus is very reasonable to assume that all clusters observed here are either nanocrystals or crystallite structures related to those of the ideal nanocrystals. Vanadium-carbide nanocrystals thus have spectra similar to those for titanium-carbide. Truncated nanocrystals have essentially the same spectra in this wavelength region as the corresponding ideal structures, and there is only a weak size-dependence for nanocrystals of different sizes.

The similarity of spectra for different sized nanocrystals may seem surprising at first glance. It seems odd that clusters with 27 atoms (i.e.,  $3 \times 3 \times 3$ ) would have the same spectra as clusters up to 64 atoms ( $4 \times 4 \times 4$ ). However, it is important to note that this measurement does not cover the entire IR spectrum. It covers only the region above  $400 \text{ cm}^{-1}$ , where relatively high frequency modes are detected. Ab initio calculations for the  $\text{M}_{14}\text{C}_{13}$  cluster indicate that these modes represent metal-carbon stretching vibrations on the surface of the cluster [30]. Since all of these clusters have essentially only surface atoms (e.g., the  $4 \times 4 \times 4$  64-atom cluster has only eight interior atoms) and the surface atoms are in very similar binding sites on all clusters, it is understandable that the surface modes would have strong intensity and similar frequencies for all sizes of these nanocrystals. Likewise, truncated nanocrystals have lost carbon atoms, but those which remain are in the same kind of structural sites. Size-dependent spectra may be found in the lower frequency region, and this will be the subject of future experiments.

#### 4. Conclusions

The results shown demonstrate the use of a tunable IR laser as an unusual but powerful ionization source for gas phase clusters. Using IR radiation, only stable neutral clusters are ionized. Here, this technique is used to investigate the stable structures of vanadium-carbide clusters. In contrast to previous suggestions about nanocrystal structures, we find in vanadium-carbides that truncated lattices with carbon vacancies are more stable than ideal ones with carbon atoms on the corners. The structural patterns described here are observed for titanium-carbide clusters as well. There, the interpretation of the mass-spectra is complicated by the wide isotope distribution of titanium together with the coincidence of the mass of the most abundant titanium isotope with the mass of four carbon atoms. In both cases it is observed that the number of carbon atoms in the crystallites is equal to or less than the number of metal atoms. Interestingly and possibly related, it is well known empirically that solid vanadium-

and titanium-carbides always appear as carbon-deficient structures [31].

The IR-REMPI spectra of these vanadium-carbide nanocrystal clusters are in many ways similar to those measured for titanium-carbide clusters. Both systems exhibit resonances near  $500\text{ cm}^{-1}$  for all nanocrystal sizes which can be associated with bulk surface phonons. In titanium-carbide, no size-dependence can be detected in the spectra, but in vanadium-carbide a slight red-shift is seen toward larger nanocrystal sizes. However, there is no discernable difference between the spectra for truncated nanocrystals missing different numbers of corner carbon atoms and their corresponding ideal structures.

### Acknowledgements

We gratefully acknowledge the support by the “Stichting voor Fundamenteel Onderzoek der materie” (FOM) in providing the required beam time of FELIX and greatly appreciate the skillful assistance of the FELIX staff. This work is part of the research program of the FOM, which is supported financially by the “Nederlandse Organisatie voor Wetenschappelijk Onderzoek” (NWO). MAD acknowledges support from the US Air Force Office of Scientific Research grant No. F49620-97-1-0042.

### References

- [1] C.L. Cleveland, U. Landman, T.G. Schaaff, M.N. Shafiqullin, P.W. Stephens, R.L. Whetten, *Phys. Rev. Lett.* 79 (1997) 1873.
- [2] Y. Volokitin, J. Sinzig, L.J. de Jongh, G. Schmid, M.N. Vargaftik, I.I. Moiseev, *Nature* 384 (1996) 621.
- [3] M. Nirmal, B.O. Dabousi, M.G. Bawendi, J.J. Macklin, J.K. Trautman, T.D. Harris, L.E. Brus, *Nature* 383 (1996) 802.
- [4] M. Bruchez, M. Moronne, P. Gin, S. Weiss, A.P. Alivisatos, *Science* 281 (1998) 2013.
- [5] S.A. Empedocles, M.G. Bawendi, *Science* 279 (1997) 2114.
- [6] G. von Helden, A.G.G.M. Tielens, D. van Heijnsbergen, M.A. Duncan, S. Hony, L.B.F.M. Waters, G. Meijer, *Science* 288 (2000) 313.
- [7] A.W. Castleman Jr., K.H. Bowen Jr., *J. Phys. Chem.* 100 (1996) 12811.
- [8] J.S. Pilgrim, M.A. Duncan, *J. Am. Chem. Soc.* 115 (1993) 9724.
- [9] M.A. Duncan, *J. Cluster Sci.* 8 (1997) 238.
- [10] F.K. Fatemi, J.D. Fatemi, L.A. Bloomfield, *Phys. Rev. Lett.* 77 (1996) 4895.
- [11] A. Amrein, R. Simpson, P. Hackett, *J. Chem. Phys.* 95 (1991) 1781.
- [12] T. Leisner, K. Athanassenas, D. Kreisler, E. Recknagel, O. Echt, *J. Chem. Phys.* 88 (1993) 9670.
- [13] E.E.B. Campbell, G. Ulmer, I.V. Hertel, *Phys. Rev. Lett.* 67 (1991) 1986.
- [14] P. Wurz, K.R. Lykke, *J. Chem. Phys.* 95 (1991) 7008.
- [15] B.D. May, S.F. Cartier, A.W. Castleman Jr., *Chem. Phys. Lett.* 242 (1995) 265.
- [16] S.F. Cartier, B.D. May, A.W. Castleman Jr., *J. Chem. Phys.* 104 (1995) 3423.
- [17] G. von Helden, I. Holleman, G.M.H. Knippels, A.F.G. van der Meer, G. Meijer, *Phys. Rev. Lett.* 79 (1997) 5234.
- [18] G. von Helden, I. Holleman, G. Meijer, B. Sartakov, *Opt. Express* 4 (1996) 46.
- [19] D. van Heijnsbergen, G. von Helden, M. Duncan, A.J.A. van Rooij, G. Meijer, *Phys. Rev. Lett.* 83 (1999) 4983.
- [20] B.C. Guo, K.P. Kearns, A.W. Castleman Jr., *Science* 255 (1992) 1411.
- [21] B.C. Guo, S. Wei, J. Purnell, S. Buzza, A.W. Castleman Jr., *Science* 256 (1992) 515.
- [22] J.S. Pilgrim, M.A. Duncan, *J. Am. Chem. Soc.* 115 (1993) 6958.
- [23] B.V. Reddy, S.N. Khanna, *J. Phys. Chem.* 98 (1994) 9446.
- [24] M.M. Rohmer, C. Bo, J.M. Poblet, *J. Am. Chem. Soc.* 117 (1995) 508.
- [25] I. Dance, *J. Am. Chem. Soc.* 118 (1996) 6309.
- [26] D. Oepts, A.F.G. van der Meer, P.W. Amersfoort, *Infrared Phys. Technol.* 36 (1995) 297.
- [27] S. Wei, B.C. Guo, J. Purnell, S. Buzza, A.W. Castleman Jr., *Science* 256 (1992) 818.
- [28] L.S. Wang, H. Cheng, *Phys. Rev. Lett.* 78 (1997) 2983.
- [29] C. Oshima, T. Aizawa, M. Wuttig, R. Souda, S. Otani, Y. Ishizawa, *Phys. Rev. B* 36 (1987) 7510.
- [30] I. Dance, to be published.
- [31] L.I. Johansson, *Surf. Sci. Rep.* 21 (1995) 177.